Acta Oceanol. Sin., 2022, Vol. 41, No. 4, P. 80–90
https://doi.org/10.1007/s13131-021-1942-8
http://www.aosocean.com
E-mail: ocean2@hyxb.org.cn

Geochemical speciation and spatial distributions of phosphorus in surface sediments from the basin of the Marcus-Wake seamounts in the western Pacific Ocean

Chao Yuan[1], Fansheng Meng[1], Xuying Yao[1], Jianyu Ni[1]*

[1] Key Laboratory of Submarine Geosciences, Second Institute of Oceanography, Ministry of Natural Resources, Hangzhou 310012, China

Received 13 November 2020; accepted 26 July 2021

Abstract

The concentrations of five forms of phosphorus (P) including exchangeable or loosely adsorbed P (Ex-P), Fe-bound P (Fe-P), authigenic P (Auth-P), detrital P (Det-P), and organic P (Org-P) from the basin among the Marcus-Wake seamounts (19.4°–24°N, 156.5°–161.5°E) in the western Pacific Ocean were quantified using a sequential extraction method (SEDEX) to investigate the distribution and sources of different P species. Concentrations of total P (TP) varied from 14.0 μmol/g to 44.1 μmol/g, with an average of (32.4±7.7) μmol/g. Inorganic phosphorus, which was the major chemical form of sedimentary P, ranged from 12.6 μmol/g to 40.6 μmol/g, while the concentration of Org-P varied between 1.38 μmol/g and 5.18 μmol/g, accounting for 83.4%–93.4% and 6.6%–16.6% of the TP, respectively. The relative proportions of the five P species followed the order of Det-P>Auth-P>Org-P>Fe-P>Ex-P. On average, Det-P was the major P sink resulted from the atmospheric input and accounted for approximately 58.9%±12.4% of the TP. Auth-P and Org-P comprised 22.8%±11.4% and 11.5%±3.0% of the TP, respectively, while Fe-P accounted for 5.1%±2.6%. Lastly, Ex-P comprised 1.6%±0.3% of the TP. Org-P exhibited a negative correlation with Fe-P and Auth-P, while Fe-P showed a positive correlation with Auth-P. This indicated that the formation of Fe-P and Auth-P was at the expense of the regeneration or remineralization of Org-P during early diagenesis. High concentrations of Det-P and Auth-P as well as a low ratio of total organic C to reactive P (TOC/Rea-P) suggested that the aeolian input may play a significant role in sedimentary P budget in the study area. Additionally, well-oxygenated bottom water and low sedimentation rate could be responsible for the low TOC/Org-P ratio in the sediment.

Key words: phosphorus speciation, SEDEX, sediments, western Pacific Ocean

Citation: Yuan Chao, Meng Fansheng, Yao Xuying, Ni Jianyu. 2022. Geochemical speciation and spatial distributions of phosphorus in surface sediments from the basin of the Marcus-Wake seamounts in the western Pacific Ocean. Acta Oceanologica Sinica, 41(4): 80–90, doi: 10.1007/s13131-021-1942-8

1 Introduction

Phosphorus (P) is an essential element in all organisms and plays a key role in various structural, genetic, and cellular components. It is an important nutrient, which limits the primary productivity through the photosynthesis of phytoplankton in the ocean. Notably, P also considerably affects climate change (Broecker, 1982; Reinhard et al., 2017), particularly on the geological time scale (Benitez-Nelson, 2000; Tyrrell, 1999). P is removed from the upper water column during photosynthesis, and subsequently settles down at the seafloor in the form of organic P. As phytoplankton and plankton die and degrade, portions of P before and after reaching the water-sediment interface are recycled back into the seawater and participate in the geochemical cycle again (Monbet et al., 2007). Thus, understanding the burial and diagenesis of P in sediment is essential to elucidate the geochemical cycle of this element.

Continental weathering of igneous and metamorphic rocks as well as soil is a primary source of P in oceanic P reservoirs. Moreover, rivers are the dominant means of transport of P from land to oceans. The riverine influx of P can be divided into the dissolved and particulate phases. The former accounts for 5%–10% of the total influx, while the latter for 90%–95% (Froelich, 1988; Ruttenberg, 2014). Riverine input of P constitutes approximately 50%–85% of the total P deposit on the continental shelf (Slomp, 2011). Furthermore, the atmospheric inputs, including volcanic ash, mineral particles, and aerosols, significantly contribute to the oceanic P reservoir. In open oceans, the flux of P entering the ocean via atmospheric deposition can reach 2×10^{10}–5×10^{10} mol/a (Ruttenberg, 2014).

Previous research on the sedimentary P geochemistry have demonstrated that P occurs in different forms in marine sediments, such as exchangeable or loosely adsorbed P (Ex-P), Fe-bound P (Fe-P), authigenic P (Auth-P), detrital P (Det-P), and organic P (Org-P). It was also found that each form is involved in different geochemical processes. Various P phases can be transformed into each other during early diagenesis in a process named "sink switching" (Ruttenberg, 2014). This Ex-P is generally considered to be bioavailable through desorption process. Amorphous iron oxyhydroxide and iron oxides show the strong capacity of adsorption for phosphate (Berner, 1973). As a result,

Foundation item: The China Ocean Mineral Resources Exploration and Development Special Foundation under contract No. DY135-S1-1-08.

*Corresponding author, E-mail: jianyuni@sio.org.cn

the iron oxides content in sediments is an important factor in regulating the P retention capacity of sediments (Zhang and Huang, 2007). Fe-P, remobilized in the oxygen-free environment, could be a source of Auth-P (Zhang et al, 2010). Authigenic carbonate fluorapatite is an abundant authigenic P phase formed by consumption of various P forms (e.g., Org-P and Fe-P) (Gächter and Meyer, 1993; Kujawinski, 2011; Ruttenberg and Berner, 1993). Organic matter is the major shuttle of P to sediments. During its degradation, phosphate is released into the porewater to undergo different biogeochemical processes, including adsorption onto particulates, binding to Fe-oxides, or incorporation into authigenic mineral lattice. However, P is ultimately buried as an authigenic carbonate fluorapatite. The decoupling of P and C is observed with sediment depth and age (Ingall et al., 1993; Filippelli and Delaney, 1996; Filippelli, 2001; Anderson et al., 2001). Det-P is generally believed insoluble and not readily bioavailable, highly connects with terrigenous input (Anderson et al, 2010). Different P forms display different biological and chemical reactivities and fates in the ocean. Hence, evaluation of the known P species is essential to provide insights into the geochemical processes of P occurring in marine sediments.

The sequential extraction (SEDEX) method has been widely employed to investigate the distributions of different P phases. Nevertheless, despite extensive research concerning the P phases in lakes and rivers (Acharya et al., 2016; Aydin et al., 2009; Berner and Rao, 1994; Eijsink et al., 2000; Fang et al., 2007; Jiang et al., 2011; Kang et al., 2017; Łukawska-Matuszewska and Burska, 2011; Yang et al., 2018), only few studies focused on open oceans, particularly the western Pacific Ocean. In this study, the abundances of five phases of P in surface sediments from the basin among the Marcus-Wake seamounts (hereafter referred to as BMW; 19.4°–24°N, 156.5°–161.5°E) in the western Pacific Ocean were determined using the SEDEX method to examine the distributions and sources of different P phases for better understanding the biogeochemical cycle of P in marine environments.

2 Materials and methods

2.1 *Regional setting*

The study area is located North Pacific subtropical gyre where soluble reactive phosphorus (SRP) was exhausted with concentrations of SRP were below 10 nmol/L (Garrison and Ellis, 2015; Martiny et al., 2019; Hashihama et al., 2009). Meanwhile, the concentrations of nitrate and nitrite (N+N) were generally below 5 nmol/L. Given both low concentrations of N+N and SRP with ratio of N+N to SRP less than 2, the region was overall nitrogen deficiency (Hashihama et al., 2009). The dust deposition had an impact on the region promoted N_2 fixation. The model show atmospheric dust inputs to the ocean is 0.5–1 g/(m^2·a) (Jickells et al., 2005). The occurrence of cold oxygen-rich Antarctic Bottom Water (AABW) made the bottom water oxygen-enriched (Emery, 2001; Kawabe and Fujio, 2010). In addition, the sediments were low in organic carbon due to the oligotrophic nature of the euphotic zone (Kong et al., 2019). Extremely rare-earth elements and yttrium (REY)-rich mud containing 6 800×10^{-6} of ΣREY has been reported nearby and Fe-Mn crusts occur on the seamounts in this area (Iijima et al., 2016; Nishi et al., 2017).

2.2 *Sample collection*

Samples were recovered from the basin of the Marcus-Wake seamounts (19.4°–24°N, 156.5°–161.5°E) using a box-corer during the DY40B cruise onboard the R/V *XIANGYANGHONG 10* during August 4 to October 20 in 2016 (Fig. 1, Table 1). The box-corer

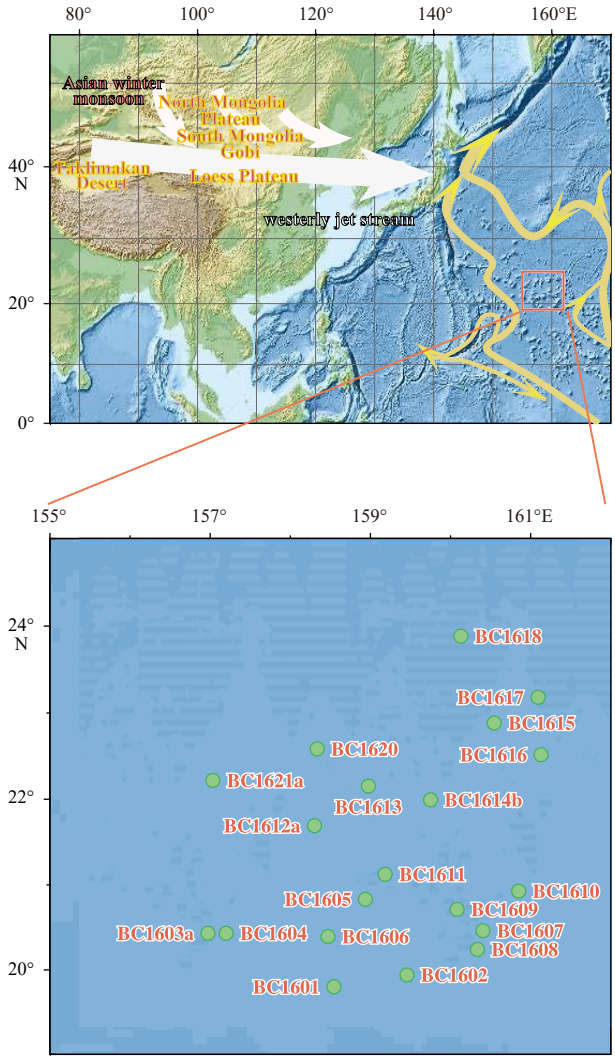

Fig. 1. Potential atmospheric P sources and sampling locations in the western Pacific Ocean. The white arrows show the combined effects of Asian winter monsoon and westerly jet stream (modified based on Miyazaki et al. (2016)). The yellow lines highlight the spreading of the Antarctic Bottom Water (Emery, 2001; Kawabe and Fujio, 2010).

samples represented approximately the top 30–50 cm of the sediment. However, only the samples from the top 2 cm were used and stored frozen until further processing in the onshore laboratory. In the laboratory, the sediment samples were freeze-dried and ground into powder (<120 mesh, 125 μm) using an agate pestle and mortar. The prepared samples were used to measure the concentrations of different P species and total organic carbon (TOC). Among the collected sediment samples, BC1604 and BC1605 were light brown diatomaceous oozes, while others were pale to reddish-brown pelagic clays.

2.3 *Sequential extraction and measurements*

The extraction steps adopted in this work followed the modified SEDEX method previously described by Ni et al. (2015). The approach was largely based on the method developed by Ruttenberg (1992) and revised by Zhang et al. (2010). Extractions of P were performed at room temperature (~22–25°C). Sedimentary P was chemically fractionated into five operationally defined P species, i.e., Ex-P, Fe-P, Auth-P (including carbonate fluorapatite,

Table 1. Sampling locations, water depths, and P concentrations (μmol/g) of total phosphorus (TP), total inorganic P (TIP), and total organic P (TOP) in dried sediment

Station	Latitude	Longitude	Depth/m	TP/(μmol·g^{-1})	TIP/(μmol·g^{-1})	TOP/(μmol·g^{-1})
BC1601	19.80°N	158.54°E	5 648	43.3	40.1	3.18
BC1602	19.94°N	159.46°E	5 502	42.8	40.0	2.81
BC1603a	20.43°N	156.97°E	5 094	34.2	31.5	2.72
BC1604	20.43°N	157.20°E	5 467	14.0	12.6	1.38
BC1605	20.83°N	158.94°E	5 574	19.9	17.4	2.52
BC1606	20.39°N	158.47°E	5 574	37.5	34.2	3.23
BC1607	20.46°N	160.40°E	5 123	37.9	34.6	3.26
BC1608	20.24°N	160.34°E	4 934	44.1	40.6	3.52
BC1609	20.71°N	160.08°E	5 645	33.8	30.3	3.49
BC1610	20.93°N	160.85°E	4 993	37.3	32.7	4.61
BC1611	21.12°N	159.18°E	5 640	29.7	26.1	3.59
BC1612a	21.69°N	158.30°E	5 149	37.1	33.1	3.92
BC1613	22.15°N	158.98°E	5 293	31.6	27.1	4.57
BC1614b	21.99°N	159.75°E	5 321	24.1	20.8	3.28
BC1615	22.88°N	160.55°E	5 564	25.3	21.7	3.59
BC1616	22.52°N	161.13°E	5 052	29.2	24.9	4.31
BC1617	23.18°N	161.09°E	5 371	29.8	26.1	3.67
BC1618	23.88°N	160.13°E	5 528	30.3	25.6	4.70
BC1620	22.58°N	158.34°E	5 443	34.1	29.5	4.60
BC1621a	22.22°N	157.03°E	5 310	31.3	26.1	5.18

biogenic Ca-P, and $CaCO_3$-bound P), Det-P of igneous and metamorphic origin, and Org-P. Total phosphorus (TP) was calculated by adding all five fractions (i.e., TP = Ex-P + Fe-P + Auth-P + Det-P + Org-P). Reactive P (Rea-P) was defined as the sum of all non-detrital fractions (i.e., Rea-P = Ex-P + Fe-P + Auth-P + Org-P). And total inorganic phosphorus (TIP) is the sum of non-organic fractions (i.e., TIP = Ex-P + Fe-P + Auth-P + Det-P).

Extractions were conducted in 50 mL polyethylene centrifuge tubes using ~0.1 g of the freeze-dried sediment and 10 mL of the extraction solution (Table 2). Following each extraction, the sample was centrifuged and the supernatant containing the extracted P was manually analyzed by the standard phosphomolybdenum blue method (Hansen and Koroleff, 1999) using a Model-7230 spectrophotometer (Shanghai Precision Instrument Company). The same medium as the one used as the extraction solution for each P species was used to prepare the standard and blank samples. The modified chromogenic reagent was prepared to avoid interference from the extraction solution (e.g., bicarbonate-dithionite extracts of Fe-P) (Zhang et al., 2010). The acidic extraction solution was neutralized and pre-treated prior to the analysis by the phosphomolybdenum blue method. The detection limit for the extracted P was 8–10 nmol/L based on the replicate blank sample measurements using 5 cm cuvettes, with a precision of >2% (Ni et al., 2015). The detailed SEDEX procedures are summarized in Table 2. Each step was followed by successive $MgCl_2$ (pH=8) and distilled water washes for 2 h at room temperature.

2.4 *Measurement of sedimentary organic carbon*

For the TOC analysis, ~0.2 g of the sediment sample was decalcified by reacting with 1 mol/L HCl. Following subsequent rinses with ultrapure water, the decalcified sample was freeze-dried. An aliquot of the sample (~20 mg) was used for the measurement of TOC on an elemental analyzer Thermo Flash EA 1112 (Milano, Italy). The precision of the TOC analysis was ±0.01%, as determined by replicate analysis of samples and Urea (Fluka, Buchs, Switzerland) as standard material.

3 Results

3.1 *Spatial variation of TP*

The total extracted P concentrations were in the range of 14.0–44.1 μmol/g, with an average of (32.3±7.7) μmol/g. The highest concentration of TP was found at station BC1601, whereas the lowest at station BC1604. In diatomaceous oozes extracted from stations BC1604 and BC1605, the TP concentrations were determined at 14.0 μmol/g and 19.9 μmol/g, respectively. Notably, these were remarkably lower than those in the pelagic clay samples. The concentrations of TP in the surface sediments showed a spatial gradient with higher values in the southeastern part of the study area and lower in the northern part (Fig. 2).

3.2 *Different P phases in the surface sediments*

The Ex-P concentrations in the surface sediments varied between 0.19 μmol/g and 0.76 μmol/g, with an average of (0.52±0.12) μmol/g, which accounted for an average of

Table 2. Details of the sequential extraction procedure

Step	Extraction	Target
1	10 mL of 1 mol/L $MgCl_2$ (pH 8), shaking for 4 h	exchangeable or loosely adsorbed P (Ex-P)
2	10 mL of BD (0.11 mol/L $NaHCO_3$+0.11 mol/L $Na_2S_2O_4$, pH 7), shaking for 6 h	reactive Fe-bound P (Fe-P)
3	10 mL of HAc/NaAc (pH 4), shaking for 6 h	authigenic P (Auth-P)
4	10 mL of 1 mol/L HCl, shaking for 16 h	detrital P (Det-P)
5	ashing at 550°C for 2 h, 10 mL of 1 mol/L HCl, shaking for 24 h	organic P (Org-P)

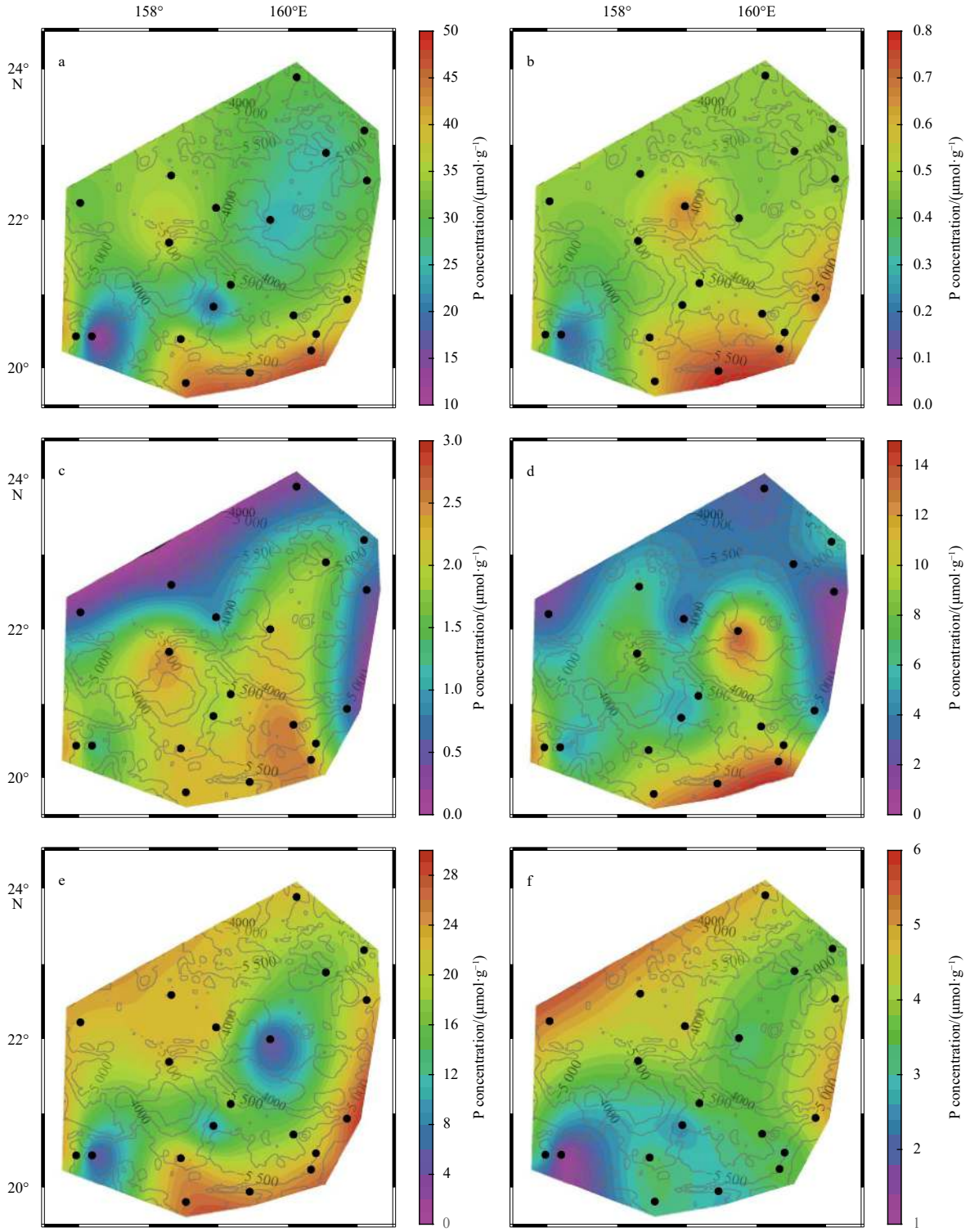

Fig. 2. Spatial distributions of different dried sedimentary P phrases, including total phosphorus (a), exchangeable or adsorbed P (b), reactive Fe-bound P (c), authigenic P (d), detrital P (e) and organic P (f), in the Marcus-Wake seamounts. The gray contours are isobaths (unit: m).

1.6%±0.3% of TP (Table 3). Moreover, Ex-P followed a spatial distribution pattern similar to that of TP, with higher values in the southern part of the study area. The lowest concentration of Ex-P was determined in the diatomaceous oozes at station BC1604 (Fig. 2). Furthermore, the Fe-P concentrations ranged from 0.38 μmol/g to 2.50 μmol/g, with an average of (1.58±0.76) μmol/g, which constituted an average of 5.1%±2.6% of TP (Table 3). Compared with the samples from the northwestern part of the study area, the Fe-P concentrations obtained from the southeastern was relatively higher (Fig. 2). The Auth-P concentrations varied from 1.74 μmol/g to 13.13 μmol/g, with an average of (7.26±3.68) μmol/g (Table 3).

Table 3. Concentrations of different sedimentary P phases including exchangeable or loosely adsorbed P (Ex-P), Fe-bound P (Fe-P), authigenic P (Auth-P), detrital P (Det-P), and organic P (Org-P) (all in μmol/g) and total organic carbon (TOC) (in mass percent, wt.%), as well as molar ratio of TOC : Org-P and TOC : Rea-P in the basin of the Marcus-Wack seamounts

Station	Ex-P	Fe-P	Auth-P	Det-P	Org-P	TOC/%	TOC : Org-P	TOC : Rea-P
BC1601	0.59	2.28	11.26	26.00	3.18	0.32	83.9	15.4
BC1602	0.76	2.26	12.90	24.11	2.81	0.26	77.1	11.6
BC1603a	0.47	2.11	10.45	18.44	2.72	0.31	95.0	16.4
BC1604	0.19	1.31	5.36	5.73	1.38	0.22	132.8	22.2
BC1605	0.50	1.86	5.16	9.87	2.52	0.24	79.4	19.9
BC1606	0.57	2.23	8.53	22.92	3.23	0.27	69.7	15.4
BC1607	0.54	1.94	10.18	21.96	3.26	0.26	66.5	13.6
BC1608	0.69	2.41	12.94	24.54	3.52	0.27	63.9	11.5
BC1609	0.56	2.50	9.31	17.89	3.49	0.25	59.7	13.1
BC1610	0.65	0.74	4.91	26.43	4.61	0.27	48.8	20.6
BC1611	0.51	1.94	6.03	17.66	3.59	0.28	65.0	19.3
BC1612a	0.49	2.41	8.50	21.74	3.92	0.26	55.3	14.1
BC1613	0.66	0.92	3.38	22.10	4.57	0.30	54.7	26.2
BC1614b	0.47	2.13	13.13	5.06	3.28	0.30	76.2	13.2
BC1615	0.47	1.72	3.85	15.67	3.59	0.28	65.0	24.2
BC1616	0.47	0.58	1.74	22.07	4.31	0.27	52.2	31.7
BC1617	0.47	0.97	5.86	18.83	3.67	0.26	59.0	19.7
BC1618	0.47	0.38	2.85	21.93	4.70	0.30	53.2	29.8
BC1620	0.47	0.53	6.36	22.14	4.60	0.29	52.5	20.2
BC1621a	0.47	0.47	2.49	22.68	5.18	0.32	51.5	31.0
Average	0.52	1.58	7.26	19.39	3.61	0.28	68.1	19.5
SD	0.12	0.76	3.68	6.11	0.90	0.03	19.7	6.4

As demonstrated in Fig. 3, Auth-P was the second largest pool of sedimentary P, constituting an average of 22.8%±11.4% of TP in the sediment of the western Pacific Ocean. The Det-P concentrations varied from 5.06 μmol/g to 26.43 μmol/g, with an average of (19.39±6.11) μmol/g (Table 3). Notably, Det-P was the largest reservoir of sedimentary P and constituted an average of 58.9%±12.4% of the TP pool. Lastly, the Org-P concentrations varied from 1.38 μmol/g to 5.18 μmol/g, with an average of (3.61±0.90) μmol/g, which accounted for an average of 11.5%±3.0% of the TP (Table 2). Compared to Fe-P and Auth-P, Org-P exhibited a reversed spatial distribution (Fig. 2).

3.3 *TOC*

Contents of TOC in the surface sediments varied from 0.22 wt.% to 0.32 wt.%, with an average of 0.28 wt.%±0.03 wt.% (Table 3). The relatively low TOC content here was attributed to the oligotrophic setting and lower primary productivity in the study area (Kong et al., 2019).

4 Discussion

It is known that the distribution of P in sediments is predominantly controlled by sedimentary rate, redox condition, grain size, contents of organic carbon and Fe/Mn oxides, and sediment characteristics (Anderson et al., 2001; Babu and Nath, 2005; Łukawska-Matuszewska and Bolałek, 2008; Łukawska-Matuszewska and Burska, 2011; März et al., 2014). In most parts of the Pacific Ocean, concentrations of TP in sediment ranged from 16 μmol/g to 98 μmol/g, while in some regions, such as central and southeastern parts of the Pacific Ocean and a smaller region near the coast of Peru, the TP concentrations reached >98 μmol/g (Baturin, 1988; Filippelli and Delaney, 1996; Kyte et al., 1993; Moody et al., 1988; Murray and Leinen, 1993; Ni et al., 2015). The average concentration of TP (32.36±7.68) μmol/g in the study area was higher than those in offshore of China, Ocean Drilling Program (ODP) 130 and 138 in equatorial Pacific Ocean and the Saanich Inlet, less than central Pacific Ocean (Fig. 4).

The TP concentrations in diatomaceous oozes at stations

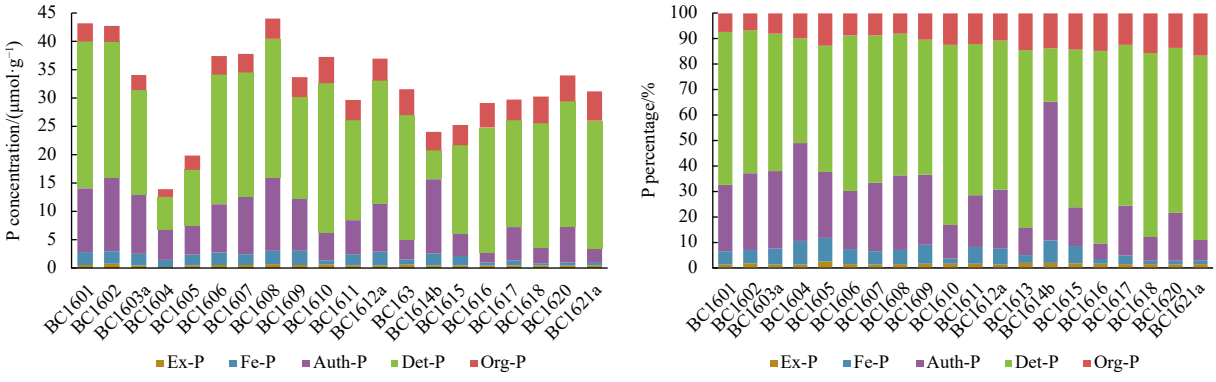

Fig. 3. Concentrations (a) and percentages (b) of five different P phases.

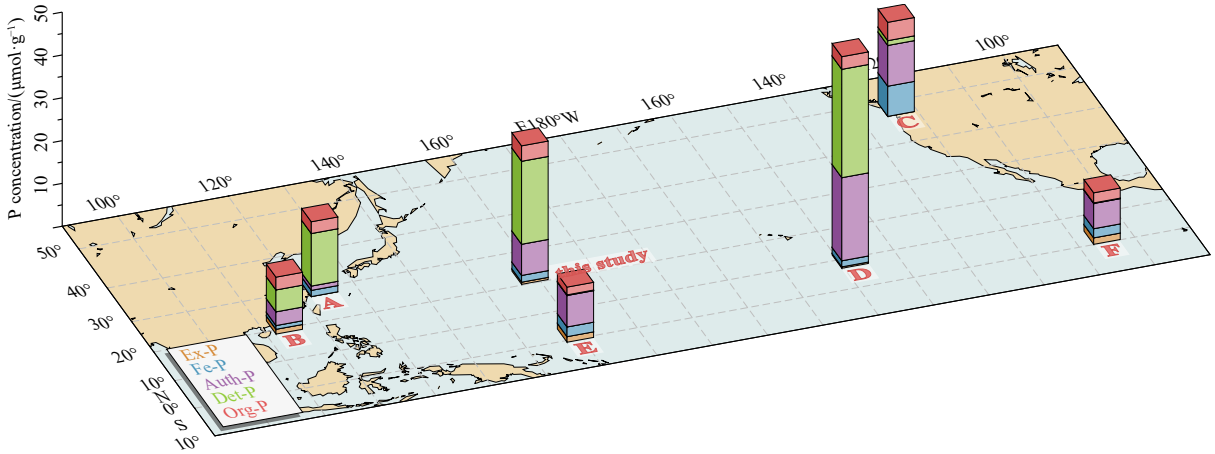

Fig. 4. Variations in the concentration and speciation of five P phases in the Pacific Ocean based on our data and other studies (data from A. Fang et al. (2007); B. Yang et al. (2018); C. Filippelli (2001); D. Ni et al. (2015); E. ODP 130, and F. ODP 138 from Filippelli and Delaney (1996)).

BC1604 and BC1605 were lower than those in pelagic clays (Table 1). This is similar to the spatial variation of the total sedimentary P in the central Indian Ocean, where higher TP concentrations were detected in the pelagic clay area (Linsy et al., 2018). The high particle reactivity of P likely promotes its adsorption onto the surfaces of fine-grained particles, such as clays and oxides/hydroxides (Lin et al., 2016; Linsy et al., 2018). Compared with pelagic clays, diatomaceous ooze typically contains coarser grains, which may be responsible for low concentration of Ex-P and Fe-P compared with that of stations in vicinity with pelagic clay (Garrison and Ellis, 2015; Fig. 2). Due to higher sedimentation rates of diatomaceous ooze compared with pelagic clay (Seibold and Berger, 2017), the accumulation time of Det-P is shorter in diatomaceous ooze station as we taken the same top 2 cm of box-corer for sample analysis. By the same token, the time either the formation *in situ* or settlement of Auth-P is shorter. Thus, the concentrations of Det-P and Auth-P in diatomaceous ooze station was lower than pelagic clay. The relative proportion of different P phases in the BMW sediment follow the order of Det-P>Auth-P>Org-P>Fe-P>Ex-P (Fig. 2). Det-P is the largest P pool in the BMW sediment, exceeding 50% of the TP, with an average of 58.9% (Fig. 2). These results differ from those determined for sediments around the equatorial Pacific Ocean (Filippelli and Delaney, 1996). Generally, P predominantly enters the ocean via rivers and atmospheric transport, with the atmospheric/aerosol input prevailing in open ocean environments, especially within the northern hemisphere "dust belt" between ~10°N and ~60°N (Prospero et al., 2002; Maher et al., 2010). Kyte et al. (1993) reported that bulk surface sediments at site LL44-GC3 in the north central Pacific contained 95% eolian dust. Previous studies also described a large proportion of Det-P related to terrigenous input in the central Pacific Ocean and the Bering Sea (März et al., 2014; Ni et al., 2015; Zhang et al., 2010). Earlier studies revealed the combined effects of the Asian winter monsoon and the westerly jet stream, which delivered terrigenous materials originating from the Taklimakan Desert, Loess Plateau, and south Mongolian Gobi Desert to the north Pacific Ocean, where the terrigenous input is the dominant component of pelagic sediments (Chen et al., 2006; Jones et al., 2000; Miyazaki et al., 2016; Yasukawa et al., 2019; Zhao et al., 2015) (Fig. 1). Hashihama et al. (2009)'s research, based on the model stimulation, showed the area (20°–30°N, 150°–160°E) existed the spike of dust deposition which contributed to elevated N_2-fixed as the result of iron supply in the region. Given the source of P in aerosols varied highly, solubility of P from different sources is greatly difference. Generally, solubility of P from mineral source is lower than particles form anthropogenic sources (Herut et al., 2002; Anderson et al., 2010; Shi et al., 2019; Herbert et al., 2018). The solubility of P in aerosols also may be related to specific P phases which have different susceptibility to dissolution (Anderson et al., 2010). Shi et al. (2019) studied phosphorus solubility in aerosol particles from westerly wind in China, and found total dissolved P constitute 21.3%±9.8% of TP in spring, the season particles mainly influenced by mineral dust form the arid and semiarid areas. And the part of soluble P may connect with anthropogenic sources (Anderson et al., 2010). Nenes et al. (2011) proposed solubility of P in aerosols increased with enhanced acidification intensity which correlated to SO_4^{2-} and NO_3^-. And pH may be seldom above 4 in aerosols only when aerosol particles were to reside in clouds and were activated into cloud droplets. Thus, Det-P may be more resistant to experience transformation than Auth-P in aerosols, due to pre-extraction step using acetate buffer (pH=4, step 3) for Auth-P before Det-P extraction in SEDEX procedure. Flaum (2008) and Guo et al. (2011) found that Det-P and Auth-P were the dominant P species in the dust from the Loess Plateau and Gobi Desert, accounting for approximately 42.5% and 41.9% of the TP, respectively. They determined that the higher concentration of Det-P was associated with finer grain size, which was easily transported by wind to the ocean. The percentage of Det-P in the sedimentary TP of the BMW (on average 59.0%) was comparable to that of the Asian eolian dust, indicating that Det-P in the study area was mainly derived from the eolian input.

Auth-P was the second largest pool of TP in the BMW (Table 2). Earlier research demonstrated that in addition to *in situ* precipitation, atmospheric input also contributed Auth-P to the sedimentary P pool (Eijsink et al., 2000; Faul et al., 2005; Kraal et al., 2012; Ni et al., 2015). The processes of degradation and dissolution of P from the reactive phases mainly controlled the *in situ* Auth-P formation. In marine sediments, Auth-P precipitates *in situ* at the expense of other P pools, particularly from organic, loosely adsorbed, and iron oxide-bound P during early diagenesis. The released and dissolved P during early diagenesis reacts with calcium, fluoride, and carbonate within the sediment. Auth-P is formed when the concentration of P is above the threshold of

precipitation (Froelich et al., 1988; Monbet et al., 2007; Paytan and McLaughlin, 2007; Vink et al., 1997). The BMW is located in the spreading path of the AABW (Fig. 1). Due to the oxygenated bottom water carried by AABW, the Fe-oxides in the surface sediments acted as competitors rather than contributors of P for upward-diffused interstitial water and effective adsorption of P (Emery, 2001; Kawabe and Fujio, 2010; Tsandev et al., 2012). Babu and Nath (2005) also established that the concentration of Auth-P was higher in the oxygen minimum zone than in oxygenated deep-sea sediments of the Arabian Sea. Hence, the oxygen-rich conditions of the BMW indicated that the *in situ* formation of Auth-P was not favorable.

The positive correlation between Auth-P and Fe-P (r^2=0.64, n=20) in BMW indicated their common origin (Fig. 5d). There are two sources control the concentration of Auth-P. One is *in situ* formation. Though the environment is not favorable, the formation of Auth-P *in situ* played an important for P sink. P released form degradation of organic matter can transform into Auth-P and the low content of TOC indicated intense remineralization of organic matter. Considering the almost same contents of TOC, the burial of organic matters in sediments may have no significant differences in different station. Organic matter undergoes prolonged deposition in water column. In this process, P is preferential mineralization, and only left refractory organic matter settled in the seafloor. As shown in Figs 5a–c, the negative correlations of Org-P & Auth-P, Org-P & Auth-P, and Org-P & (Auth-P + Fe-P) indicated the *in situ* formations of carbonate fluorapatite (part of Auth-P) and Fe-P had been a certain extent to which P released from Org-P transferred into Auth-P and Fe-P, as Ruttenberg and Berner (1993) reported before. The deviation of the diatomaceous ooze samples from the major linear trend of pelagic clay samples may be caused by the high sedimentation rate and shorter diagenetic time (Fig. 3).

Still, *in situ* formation is only one factor conditioning the concentrations of Auth-P in this area. Atmospheric input significantly affects the concentration of Auth-P in open oceans (Anderson et al., 2010; Mahowald et al., 2008). Guo et al. (2011) reported different P phases in the sand particles from the western Inner Mongolia utilizing the SEDEX procedure. It was determined that Auth-P was the main component of the TP with an average concentration of 16.8 μmol/g. However, most terrigenous Auth-P was in the form of weakly soluble or not bioavailable P in seawater (Anderson et al., 2010). Shi et al. (2019) also reported that the solubility of P in aerosol particles was 32.9%±16.7% and 21.3%±9.8% based on samples collected in the winter and spring of 2013, respectively. Aerosol P is commonly bound to Fe-oxides or associated with Al, Mg, or Ca, which all exhibit poor solubility in seawater (Paytan and McLaughlin, 2007). In this area, the ratio of TOC/Rea-P was generally lower than 20 (Fig. 6), similar to the central Pacific Ocean and the central Indian Basin which both affected by terrigenous inputs carrying the calcium fluorapatite into the ocean (Ni et al., 2015; Linsy et al., 2018). And the concentration of Det-P was higher than most area presented in Fig. 4 with the exception of central Pacific Ocean. Hence, it was speculated that eolian dust might considerably contribute to the Auth-P pool in the BMW. This hypothesis is in agreement with a previous finding, which showed that 63% of the Auth-P was associated with atmospheric input in the central Pacific Ocean (Ni et al., 2015). There is no significant correlation between Auth-P and Det-P which may be caused for two reasons: (1) the nature of Auth-P, formed in either the arid-alkaline environment or low pH and moist soils which is different from that formed in marine

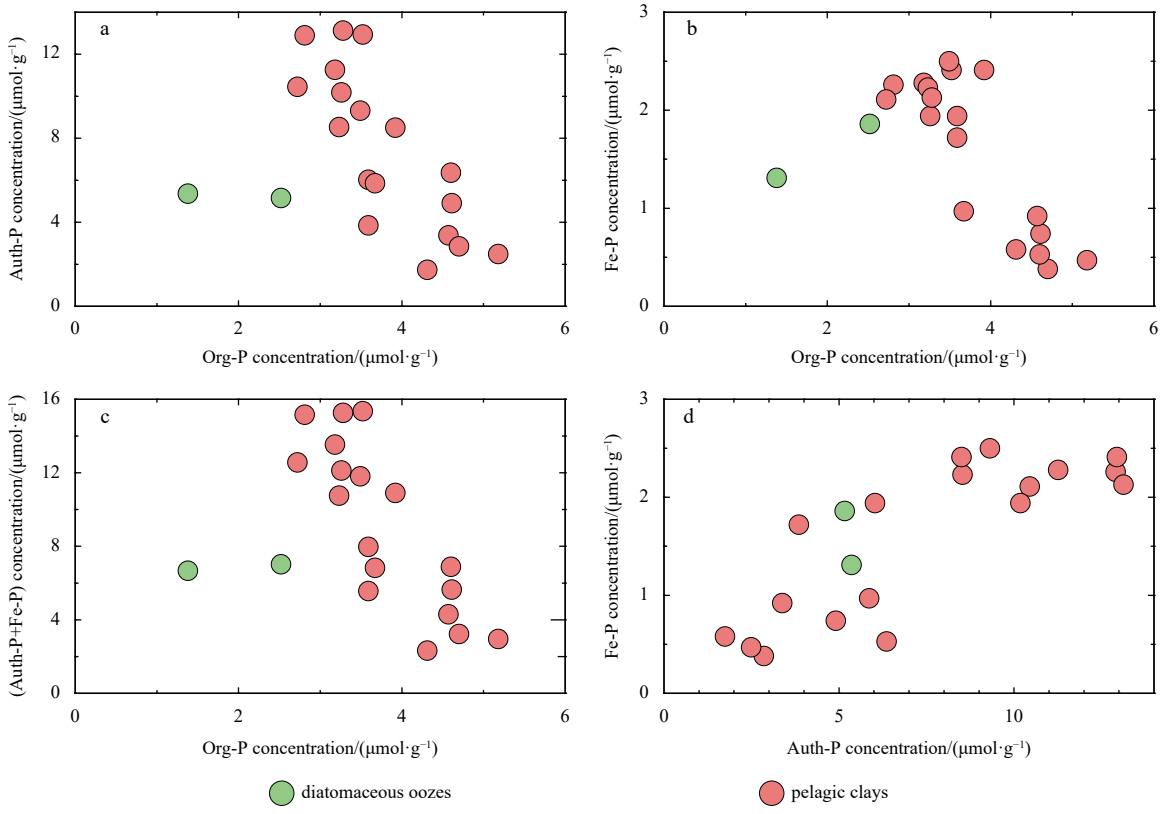

Fig. 5. Concentrations of organic P (Org-P) versus authigenic P (Auth-P) (a), Fe-bound (Fe-P) (b), the sum of Auth-P and Fe-P (c), and concentrations of Auth-P versus Fe-P (d).

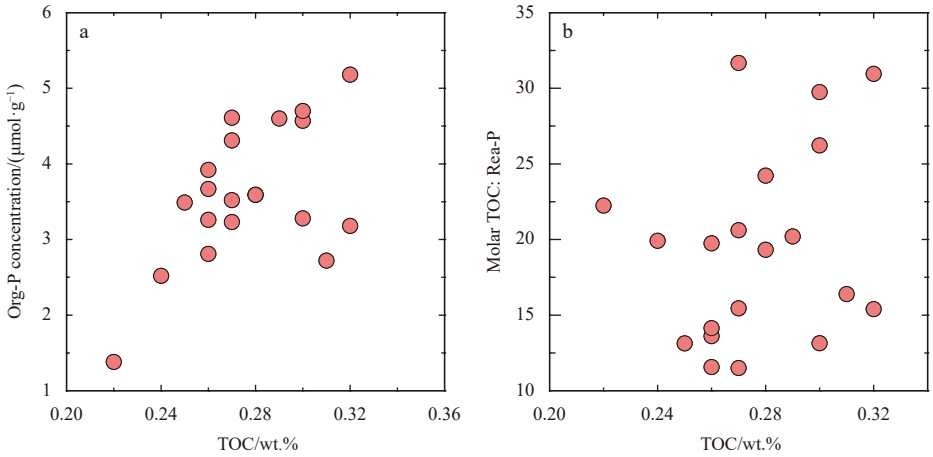

Fig. 6. The content of TOC versus organic P (Org-P) concentration (a), and molar TOC : Rea-P ratios (b) in the basin of the Marcus-Wake seamounts.

sediments, may influenced the solubility of Auth-P (Anderson et al., 2010). Part of Auth-P from continent is soluble either in seawater or aerosols while Det-P may not. (2) Auth-P formed *in situ* by consuming P released from degradation of Org-P which may mineralized by microorganisms which may varied in different stations (Ruttenberg and Berner, 1993).

Org-P constituted the third largest pool of TP in the BMW sediments (Fig. 3) and contributed an average of 11.5%±3.0% to the TP. Organic matter is the major shuttle of P to sediment. During its degradation, phosphate is released to the porewater, which subsequently undergoes various biogeochemical processes (Filippelli and Delaney, 1994; Ingall and Jahnke, 1994). In an oxic environment, the most labile organic matter undergoes degradation within the water column, resulting in low Org-P and TOC content in sediments (Ni et al., 2015). That may have responsibility for low content of TOC. In addition, a weak correlation between TOC and Org-P suggested variations in the source and state of organic matter degradation (Ni et al., 2015).

The molar TOC/Org-P and TOC/Rea-P ratios in the sediments can be affected by the redox conditions and diagenetic redistribution of organic matter. In oxic oceanic environments, most of the labile organic carbon and P can be regenerated in the water column prior to reaching the sediment. This leads to a low Org-P concentrations (on average 3.6%±0.9% of the TP) and low TOC contents (on average just 0.28 wt.%±0.03 wt.% of dried sediment) in the sediments of the study area. It is noteworthy that previous studies determined that burial of Org-P is not the largest P sink in the deep ocean (Filippelli and Delaney, 1996; Delaney, 1998). In the present study, the TOC contents exhibited an overall weak correlation with the Org-P concentrations (Fig. 6). This was consistent with previous findings in the regions characterized by low TOC content and sedimentation rates (Ingall and Van Cappellen, 1990; de Lange, 1992). The molar TOC/Org-P ratio of the BMW sediments varied from 50 to 133 (an average of 68), with the highest ratios in diatomaceous ooze (Table 2). The lower ratios were consistent with other slowly deposited pelagic sediments, e.g., the TOC/Org-P ratios of 49–63 reported by Ingall and Van Cappellen (1990). Anderson et al. (2001) and Algeo and Ingall (2007) found that the TOC/Org-P ratios could reflect the redox conditions in bottom waters and sediments, since the TOC/Org-P ratios were lower than or equal to the Redfield ratio under oxic conditions, but higher than the Redfield ratio in anoxic environments. Higher organic C/P ratios indicated the preferential loss of P during early diagenesis and the degradation of organic matter. Furthermore, Ingall and Van Cappellen (1990) related the TOC/Org-P ratios to the sediment accumulation rate. It was found that the TOC/Org-P ratios were close to the Redfield ratio in areas exhibiting the lowest sedimentation rates due to the higher concentration of refractory Org-P in residual organic matter and/or organic matter produced *in situ* from bacterial biomass. Hence, the low TOC/Org-P ratios in our sediments (sedimentation rate of 1.79 mm/ka; Yang et al., 2020) were attributed to extensive degradation of organic matter, low sedimentation ratios in the area, and long exposure to oxygen.

The ratio of TOC/Rea-P could be affected by the original C/P ratio of the organic matter buried in the sediments (Anderson et al., 2001). The addition of Auth-P and Fe-P via atmospheric input increased the concentrations of Rea-P, which might have led to the low value of TOC/Rea-P.

In oceanic environments, the transport of P from the upper water column to the seafloor is predominantly in the organic form, with additional contributions from the detrital and authigenic forms as well as P bound to Fe (oxyhydr) oxides and that adsorbed on particle surfaces (Föllmi, 1996; Paytan et al., 2003). During their settling, various forms of sedimentary P, including loosely adsorbed, Fe-bound, and organic P, might be readily released to ambient water through desorption, reductive dissolution, and degradation. It was determined that in pelagic clay environments, below the carbonate compensation depth and at low sedimentation rates, most of organic P and P-associated biogenic carbonate particles were regenerated and dispersed into the water column during settling to the seafloor or surface sediments (Zhou and Kyte, 1992). Compared to other marine environments, the BWM appeared to display relatively low adsorbed-P, Fe-P, and Org-P concentrations (Fig. 6), indicating that most of the labile P could have been released into the water column during its long transport from the surface to the seafloor and/or during early diagenesis in the sediment.

5 Conclusions

The SEDEX method was employed to quantify the abundances of five different sedimentary P species in the basin of the Marcus-Wake seamounts and to investigate their sources and distributions. The relative proportions of different P species in the study area followed the order of Det-P>Auth-P>Org-P>Fe-P>Ex-P. The concentrations of TP varied from 14.0 μmol/g to

44.1 μmol/g. TIP constituted the largest proportion of the TP, varied from 12.6 μmol/g to 40.6 μmol/g and accounted for 83.4%–93.4% of the TP. Det-P was the major P pool in the BMW, constituted for 21.0%–75.7% of the TP. Moreover, Auth-P was the second largest P pool, accounted for 6.0%–54.6% of TP. The concentrations of Org-P and Fe-P in the BMW sediments accounted for 6.6%–16.6% and 1.3%–9.4% of the TP, respectively. Lastly, the Ex-P only constituted 1.3%–2.5% of the TP. In addition, concentrations of TP in diatomaceous ooze (stations BC1604 and BC1605) were lower than those in pelagic clays due to the higher sedimentary rates and coarser particles of the former.

Compared with other area in the Pacific Ocean, the basin of Marcus-Wake had relatively high concentration of Det-P, suggesting the atmospheric inputs influencing the sedimentary P. Furthermore, atmospheric inputs carrying terrigenous P-containing materials, as well as *in situ* formation, have both contributed to Auth-P sink in the area.

Overall, a low sedimentation rates and well-oxygenated bottom waters in BMW resulted in prolonged degradation of organic matter in the water column, eventually leading to a low TOC/Org-P ratio.

The study of different P phases could support the further research of mechanism of phosphatization of Fe-Mn crusts and strong correlation between REY and biogenic calcium phosphate (Tanaka et al., 2020).

Acknowledgements

We thank the captain, crew and science teams of the R/V *XIANGYANGHONG 10* for their skillful support during sediment sampling in the Pacific Ocean. We also thank Laodong Guo at University of Wisconsin-Milwaukee and anonymous reviewers for their constructive comments that improved the manuscript significantly. Figures 1, 2 and 4–6 were drawn using the GMT package developed by Wessel et al. (2013).

References

Acharya S S, Panigrahi M K, Kurian J, et al. 2016. Speciation of phosphorus in the continental shelf sediments in the Eastern Arabian Sea. Continental Shelf Research, 115: 65–75, doi: 10.1016/j.csr.2016.01.005

Algeo T J, Ingall E. 2007. Sedimentary C_{org}: P ratios, paleocean ventilation, and Phanerozoic atmospheric pO_2. Palaeogeography, Palaeoclimatology, Palaeoecology, 256(3–4): 130–155, doi: 10.1016/j.palaeo.2007.02.029

Anderson L D, Delaney M L, Faul K L. 2001. Carbon to phosphorus ratios in sediments: Implications for nutrient cycling. Global Biogeochemical Cycles, 15(1): 65–79, doi: 10.1029/2000gb001270

Anderson L D, Faul K L, Paytan A. 2010. Phosphorus associations in aerosols: What can they tell us about P bioavailability?. Marine Chemistry, 120(1–4): 44–56, doi: 10.1016/j.marchem.2009.04.008

Aydin I, Aydin F, Saydut A, et al. 2009. A sequential extraction to determine the distribution of phosphorus in the seawater and marine surface sediment. Journal of Hazardous Materials, 168(2–3): 664–669, doi: 10.1016/j.jhazmat.2009.02.095

Babu C P, Nath B N. 2005. Processes controlling forms of phosphorus in surficial sediments from the eastern Arabian Sea impinged by varying bottom water oxygenation conditions. Deep-Sea Research Part II: Topical Studies in Oceanography, 52(14–15): 1965–1980, doi: 10.1016/j.dsr2.2005.06.004

Baturin G N. 1988. Disseminated phosphorus in oceanic sediments — A review. Marine Geology, 84(1–2): 95–104, doi: 10.1016/0025-3227(88)90127-2

Benitez-Nelson C R. 2000. The biogeochemical cycling of phosphorus in marine systems. Earth-Science Reviews, 51(1–4): 109–135, doi: 10.1016/s0012-8252(00)00018-0

Berner R A. 1973. Phosphate removal from sea water by adsorption on volcanogenic ferric oxides. Earth and Planetary Science Letters, 18(1): 77–86, doi: 10.1016/0012-821X(73)90037-X

Berner R A, Rao J L. 1994. Phosphorus in sediments of the Amazon River and estuary: Implications for the global flux of phosphorus to the sea. Geochimica et Cosmochimica Acta, 58(10): 2333–2339, doi: 10.1016/0016-7037(94)90014-0

Broecker W S. 1982. Glacial to interglacial changes in ocean chemistry. Progress in Oceanography, 11(2): 151–197, doi: 10.1016/0079-6611(82)90007-6

Chen Hungyu, Fang T H, Preston M R, et al. 2006. Characterization of phosphorus in the aerosol of a coastal atmosphere: Using a sequential extraction method. Atmospheric Environment, 40(2): 279–289, doi: 10.1016/j.atmosenv.2005.09.051

Delaney M L. 1998. Phosphorus accumulation in marine sediments and the oceanic phosphorus cycle. Global Biogeochemical Cycles, 12(4): 563–572, doi: 10.1029/98GB02263

de Lange G J. 1992. Distribution of various extracted phosphorus compounds in the interbedded turbiditic/pelagic sediments of the Madeira Abyssal Plain, eastern North Atlantic. Marine Geology, 109(1–2): 115–139, doi: 10.1016/0025-3227(92)90224-6

Eijsink L M, Krom M D, Herut B. 2000. Speciation and burial flux of phosphorus in the surface sediments of the Eastern Mediterranean. American Journal of Science, 300(6): 483–503, doi: 10.2475/ajs.300.6.483

Emery W J. 2001. Water types and water masses. In: Steele J H, Thorpe S A, Turekian K K, eds. Encyclopedia of Ocean Sciences. San Diego, CA: Academic Press, 3179–3187

Fang T H, Chen J L, Huh C A. 2007. Sedimentary phosphorus species and sedimentation flux in the East China Sea. Continental Shelf Research, 27(10–11): 1465–1476, doi: 10.1016/j.csr.2007.01.011

Faul K L, Paytan A, Delaney M L. 2005. Phosphorus distribution in sinking oceanic particulate matter. Marine Chemistry, 97(3–4): 307–333, doi: 10.1016/j.marchem.2005.04.002

Filippelli G M. 2001. Carbon and phosphorus cycling in anoxic sediments of the Saanich Inlet, British Columbia. Marine Geology, 174(1–4): 307–321, doi: 10.1016/s0025-3227(00)00157-2

Filippelli G M, Delaney M L. 1994. The oceanic phosphorus cycle and continental weathering during the Neogene. Paleoceanography, 9(5): 643–652, doi: 10.1029/94pa01453

Filippelli G M, Delaney M L. 1996. Phosphorus geochemistry of equatorial Pacific sediments. Geochimica et Cosmochimica Acta, 60(9): 1479–1495, doi: 10.1016/0016-7037(96)00042-7

Flaum J A. 2008. Investigation of phosphorus cycle dynamics associated with organic carbon burial in modern (North Pacific) and ancient (Devonian and Cretaceous) marine systems; strengths and limitations of sequentially extracted (SEDEX) phosphorus data [dissertation]. Evanston: Northwestern University

Föllmi K B. 1996. The phosphorus cycle, phosphogenesis and marine phosphate-rich deposits. Earth-Science Reviews, 40(1–2): 55–124, doi: 10.1016/0012-8252(95)00049-6

Froelich P N. 1988. Kinetic control of dissolved phosphate in natural rivers and estuaries: A primer on the phosphate buffer mechanism. Limnology and Oceanography, 33(4part2): 649–668, doi: 10.4319/lo.1988.33.4part2.0649

Froelich P N, Arthur M A, Burnett W C, et al. 1988. Early diagenesis of organic matter in Peru continental margin sediments: Phosphorite precipitation. Marine Geology, 80(3–4): 309–343, doi: 10.1016/0025-3227(88)90095-3

Gächter R, Meyer J S. 1993. The role of microorganisms in mobilization and fixation of phosphorus in sediments. Hydrobiologia, 253(1–3): 103–121, doi: 10.1007/bf00050731

Garrison T, Ellis R. 2015. Oceanography: An Invitation to Marine Science. 9th ed. Boston, MA: Cengage Learning, 139–165, 255

Guo Boshu, Yang Hongwei, Li Yan. 2011. The speciation of phosphorus in the sand particles in Western Inner Mongolia. In: Proceedings of the Second International Conference on Mechanic Automation and Control Engineering. Inner Mongolia: IEEE, 2755–2757

Hansen H P, Koroleff F. 1999. Determination of nutrients. In:

Grasshoff K, Kremling K, Ehrhardt M, eds. Methods of Seawater Analysis. Weinheim: Wiley, 159–228

Hashihama F, Furuya K, Kitajima S, et al. 2009. Macro-scale exhaustion of surface phosphate by dinitrogen fixation in the western North Pacific. Geophysical Research Letters, 36(3): L03610, doi: 10.1029/2008GL036866

Herbert R J, Krom M D, Carslaw K S, et al. 2018. The effect of atmospheric acid processing on the global deposition of bioavailable phosphorus from dust. Global Biogeochemical Cycles, 32(9): 1367–1385, doi: 10.1029/2018GB005880

Herut B, Collier R, Krom M D. 2002. The role of dust in supplying nitrogen and phosphorus to the southeast Mediterranean. Limnology and Oceanography, 47(3): 870–878, doi: 10.4319/lo.2002.47.3.0870

Iijima K, Yasukawa K, Fujinaga K, et al. 2016. Discovery of extremely REY-rich mud in the western North Pacific Ocean. Geochemical Journal, 50(6): 557–573, doi: 10.2343/geochemj.2.0431

Ingall D, Bustin R M, Van Cappellen P. 1993. Influence of water column anoxia on the burial and preservation of carbon and phosphorus in marine shales. Geochimica et Cosmochimica Acta, 57(2): 303–316, doi: 10.1016/0016-7037(93)90433-W

Ingall E, Jahnke R. 1994. Evidence for enhanced phosphorus regeneration from marine sediments overlain by oxygen depleted waters. Geochimica et Cosmochimica Acta, 58(11): 2571–2575, doi: 10.1016/0016-7037(94)90033-7

Ingall E D, Van Cappellen P. 1990. Relation between sedimentation rate and burial of organic phosphorus and organic carbon in marine sediments. Geochimica et Cosmochimica Acta, 54(2): 373–386, doi: 10.1016/0016-7037(90)90326-g

Jiang Cuihong, Hu Jiwei, Huang Xianfei, et al. 2011. Phosphorus speciation in sediments of Lake Hongfeng, China. Chinese Journal of Oceanology and Limnology, 29(1): 53–62, doi: 10.1007/s00343-011-9047-4

Jickells T D, An Z S, Andersen K K, et al. 2005. Global iron connections between desert dust, ocean biogeochemistry, and climate. Science, 308(5718): 67–71, doi: 10.1126/science.1105959

Jones C E, Halliday A N, Rea D K, et al. 2000. Eolian inputs of lead to the North Pacific. Geochimica et Cosmochimica Acta, 64(8): 1405–1416, doi: 10.1016/s0016-7037(99)00439-1

Kang Xuming, Song Jinming, Yuan Huamao, et al. 2017. Phosphorus speciation and its bioavailability in sediments of the Jiaozhou Bay. Estuarine, Coastal and Shelf Science, 188: 127–136, doi: 10.1016/j.ecss.2017.02.029

Kawabe M, Fujio S. 2010. Pacific Ocean circulation based on observation. Journal of Oceanography, 66(3): 389–403, doi: 10.1007/s10872-010-0034-8

Kong Fanping, Dong Qing, Xiang Kunsheng, et al. 2019. Spatiotemporal variability of remote sensing ocean net primary production and major forcing factors in the tropical eastern Indian and western Pacific Ocean. Remote Sensing, 11(4): 391, doi: 10.3390/rs11040391

Kraal P, Slomp C P, Reed D C, et al. 2012. Sedimentary phosphorus and iron cycling in and below the oxygen minimum zone of the northern Arabian Sea. Biogeosciences, 9(7): 2603–2624, doi: 10.5194/bg-9-2603-2012

Kujawinski E B. 2011. The impact of microbial metabolism on marine dissolved organic matter. Annual Review of Marine Science, 3(1): 567–599, doi: 10.1146/annurev-marine-120308-081003

Kyte F T, Leinen M, Heath G R, et al. 1993. Cenozoic sedimentation history of the central North Pacific: Inferences from the elemental geochemistry of core LL44-GPC3. Geochimica et Cosmochimica Acta, 57(8): 1719–1740, doi: 10.1016/0016-7037(93)90109-a

Lin Peng, Klump J V, Guo Laodong. 2016. Dynamics of dissolved and particulate phosphorus influenced by seasonal hypoxia in Green Bay, Lake Michigan. Science of the Total Environment, 541: 1070–1082, doi: 10.1016/j.scitotenv.2015.09.118

Linsy P, Nath B N, Mascarenhas-Pereira M B L, et al. 2018. Distribution and diagenesis of phosphorus in the deep-sea sediments of the Central Indian Basin. Journal of Geophysical Research: Oceans, 123(11): 7963–7982, doi: 10.1029/2018JC014386

Łukawska-Matuszewska K, Bolałek J. 2008. Spatial distribution of phosphorus forms in sediments in the Gulf of Gdańsk (southern Baltic Sea). Continental Shelf Research, 28(7): 977–990, doi: 10.1016/j.csr.2008.01.009

Łukawska-Matuszewska K, Burska D. 2011. Phosphate exchange across the sediment-water interface under oxic and hypoxic/anoxic conditions in the southern Baltic Sea. Oceanological and Hydrobiological Studies, 40(2): 57–71, doi: 10.2478/s13545-011-0017-4

Maher B A, Prospero J M, Mackie D, et al. 2010. Global connections between aeolian dust, climate and ocean biogeochemistry at the present day and at the last glacial maximum. Earth-Science Reviews, 99(1–2): 61–97, doi: 10.1016/j.earscirev.2009.12.001

Mahowald N, Jickells T D, Baker A R, et al. 2008. Global distribution of atmospheric phosphorus sources, concentrations and deposition rates, and anthropogenic impacts. Global Biogeochemical Cycles, 22(4): GB4026, doi: 10.1029/2008gb003240

Martiny A C, Lomas M W, Fu Weiwei, et al. 2019. Biogeochemical controls of surface ocean phosphate. Science Advances, 5(8): eaax0341, doi: 10.1126/sciadv.aax0341

März C, Poulton S W, Wagner T, et al. 2014. Phosphorus burial and diagenesis in the central Bering Sea (Bowers Ridge, IODP Site U1341): Perspectives on the marine P cycle. Chemical Geology, 363: 270–282, doi: 10.1016/j.chemgeo.2013.11.004

Miyazaki T, Kimura J I, Katakuse M. 2016. Geochemical records from loess deposits in Japan over the last 210 kyr: Lithogenic source changes and paleoclimatic indications. Geochemistry, Geophysics, Geosystems, 17(7): 2745–2761, doi: 10.1002/2016GC006322

Monbet P, Brunskill G J, Zagorskis I, et al. 2007. Phosphorus speciation in the sediment and mass balance for the central region of the Great Barrier Reef continental shelf (Australia). Geochimica et Cosmochimica Acta, 71(11): 2762–2779, doi: 10.1016/j.gca.2007.03.025

Moody J B, Chaboudy L R, Worsley T R. 1988. Pacific pelagic phosphorus accumulation during the last 10 M.Y. Paleoceanography, 3(1): 113–136, doi: 10.1029/pa003i001p00113

Murray R W, Leinen M. 1993. Chemical transport to the seafloor of the equatorial Pacific Ocean across a latitudinal transect at 135°W: Tracking sedimentary major, trace, and rare earth element fluxes at the Equator and the Intertropical Convergence Zone. Geochimica et Cosmochimica Acta, 57(17): 4141–4163, doi: 10.1016/0016-7037(93)90312-K

Nenes A, Krom M D, Mihalopoulos N, et al. 2011. Atmospheric acidification of mineral aerosols: a source of bioavailable phosphorus for the oceans. Atmospheric Chemistry and Physics, 11(13): 6265–6272, doi: 10.5194/acp-11-6265-2011

Ni Jianyu, Lin Peng, Zhen Yang, et al. 2015. Distribution, source and chemical speciation of phosphorus in surface sediments of the central Pacific Ocean. Deep-Sea Research Part I: Oceanographic Research Papers, 105: 74–82, doi: 10.1016/j.dsr.2015.08.008

Nishi K, Usui A, Nakasato Y, et al. 2017. Formation age of the dual structure and environmental change recorded in hydrogenetic ferromanganese crusts from Northwest and Central Pacific seamounts. Ore Geology Reviews, 87: 62–70, doi: 10.1016/j.oregeorev.2016.09.004

Paytan A, Cade-Menun B J, McLaughlin K, et al. 2003. Selective phosphorus regeneration of sinking marine particles: evidence from 31P-NMR. Marine Chemistry, 82(1–2): 55–70, doi: 10.1016/s0304-4203(03)00052-5

Paytan A, McLaughlin K. 2007. The oceanic phosphorus cycle. Chemical Reviews, 107(2): 563–576, doi: 10.1021/cr0503613

Prospero J M, Ginoux P, Torres O, et al. 2002. Environmental characterization of global sources of atmospheric soil dust identified with the Nimbus 7 Total Ozone Mapping Spectrometer (TOMS) absorbing aerosol product. Reviews of Geophysics, 40(1): 1002, doi: 10.1029/2000rg000095

Reinhard C T, Planavsky N J, Gill B C, et al. 2017. Evolution of the global phosphorus cycle. Nature, 541(7637): 386–389, doi: 10.1038/nature20772

Ruttenberg K C. 1992. Development of a sequential extraction meth-

od for different forms of phosphorus in marine sediments. Limnology and Oceanography, 37(7): 1460–1482, doi: 10.4319/lo.1992.37.7.1460

Ruttenberg K C. 2014. The global phosphorus cycle. In: Turekian K K, ed. Treatise on Geochemistry. 2th ed. Oxford: Elsevier, 499–558

Ruttenberg K C, Berner R A. 1993. Authigenic apatite formation and burial in sediments from non-upwelling, continental margin environments. Geochimica et Cosmochimica Acta, 57(5): 991–1007, doi: 10.1016/0016-7037(93)90035-u

Seibold E, Berger W. 2017. The Sea Floor: An Introduction to Marine Geology. 4th ed. Berlin: Springer

Shi Jinhui, Wang Nan, Gao Huiwang, et al. 2019. Phosphorus solubility in aerosol particles related to particle sources and atmospheric acidification in Asian continental outflow. Atmospheric Chemistry and Physics, 19(2): 847–860, doi: 10.5194/acp-19-847-2019

Slomp C P. 2011. Phosphorus cycling in the estuarine and coastal zones: Sources, sinks, and transformations. In: Wolanski E, McLusky D S, eds. Treatise on Estuarine and Coastal Science. London: Academic Press, 201–229

Tanaka E, Nakamura K, Yasukawa K, et al. 2020. Chemostratigraphy of deep-sea sediments in the western North Pacific Ocean: Implications for genesis of mud highly enriched in rare-earth elements and yttrium. Ore Geology Reviews, 119: 103392, doi: 10.1016/j.oregeorev.2020.103392

Tsandev I, Reed D C, Slomp C P. 2012. Phosphorus diagenesis in deep-sea sediments: Sensitivity to water column conditions and global scale implications. Chemical Geology, 330–331: 127–139, doi: 10.1016/j.chemgeo.2012.08.012

Tyrrell T. 1999. The relative influences of nitrogen and phosphorus on oceanic primary production. Nature, 400(6744): 525–531, doi: 10.1038/22941

Vink S, Chambers R M, Smith S V. 1997. Distribution of phosphorus in sediments from Tomales Bay, California. Marine Geology, 139(1–4): 157–179, doi: 10.1016/s0025-3227(96)00109-0

Wessel P, Smith W H F, Scharroo R, et al. 2013. Generic mapping tools: Improved version released. Eos, Transactions American Geophysical Union, 94(45): 409–410, doi: 10.1002/2013EO450001

Yang Bin, Liu Sumei, Zhang Guoling. 2018. Geochemical characteristics of phosphorus in surface sediments from the continental shelf region of the northern South China Sea. Marine Chemistry, 198: 44–55, doi: 10.1016/j.marchem.2017.11.001

Yang Zifei, Qian Qiankun, Chen Min, et al. 2020. Enhanced but highly variable bioturbation around seamounts in the northwest Pacific. Deep-Sea Research Part I: Oceanographic Research Papers, 156: 103190, doi: 10.1016/j.dsr.2019.103190

Yasukawa K, Ohta J, Miyazaki T, et al. 2019. Statistic and isotopic characterization of deep-sea sediments in the western North Pacific Ocean: Implications for genesis of the sediment extremely enriched in rare earth elements. Geochemistry, Geophysics, Geosystems, 20(7): 3402–3430, doi: 10.1029/2019GC008214

Zhang Jiazhong, Guo Laodong, Fischer C J. 2010. Abundance and chemical speciation of phosphorus in sediments of the Mackenzie River Delta, the Chukchi Sea and the Bering Sea: Importance of detrital apatite. Aquatic Geochemistry, 16(3): 353–371, doi: 10.1007/s10498-009-9081-4

Zhang Jiazhong, Huang Xiaolan. 2007. Relative importance of solid-phase phosphorus and iron on the sorption behavior of sediments. Environment Science & Technology, 41(8): 2789–2795, doi: 10.1021/es061836q

Zhao Wancang, Sun Youbin, Balsam W, et al. 2015. Clay-sized Hf-Nd-Sr isotopic composition of Mongolian dust as a fingerprint for regional to hemispherical transport. Geophysical Research Letters, 42(13): 5661–5669, doi: 10.1002/2015GL064357

Zhou Lei, Kyte F T. 1992. Sedimentation history of the South Pacific pelagic clay province over the last 85 million years inferred from the geochemistry of Deep Sea Drilling Project Hole 596. Paleoceanography, 7(4): 441–465, doi: 10.1029/92pa01063